

Simulation study on number of secondary particles in extensive air showers using CORSIKA codeS. M. H. Halataei,¹ M. Bahmanabadi,^{1,2,*} M. Khakian Ghomi,² and J. Samimi^{1,2}¹*Department of Physics, Sharif University of Technology, P.O. Box 11365-9161, Tehran, Iran*²*ALBORZ Observatory, Sharif University of Technology, Tehran, Iran*

(Received 7 November 2007; published 7 April 2008)

We have simulated more than 10^5 extensive air showers (EAS) by CORSIKA code, with a proton as the primary particle. The range of energy for primary particles was selected from 50 TeV to 5 PeV, with differential flux given by $dN/dE \propto E^{-2.7}$. Using the secondary charged particles produced of these EASs, we obtained the function $dN_{\text{sp}}(\theta, X)/d\theta$, where $N_{\text{sp}}(\theta, X)$ is the number of secondary charged particles in EASs as a function of atmosphere depth, X , and zenith angle, θ . A $\sin\theta\cos^{n(X)}\theta$ distribution was obtained for zenith angle distribution of the number of secondary charged particles, where power index, $n(X)$, is a function of atmosphere depth, X . We obtained $n(X) = 3.02 + 0.003X \ln X - 8.28 \times 10^{-9}X^3 - 1.35 \ln X$. We have compared our results with the experimental data of various observatories.

DOI: [10.1103/PhysRevD.77.083001](https://doi.org/10.1103/PhysRevD.77.083001)

PACS numbers: 96.50.sd, 95.75.-z, 96.50.S-

I. INTRODUCTION

When high energy cosmic rays (gammas, protons, or heavy nuclei) impinge onto the Earth's atmosphere, they interact at high altitude with the air nuclei as targets. By repeated interaction of the secondaries an extensive air shower (EAS) is generated. Investigation of gamma rays and cosmic rays in the energy ranges about 100 TeV needs to investigate EAS events. From the EAS investigations, in addition to the extraction of some information like direction, type, and energy of the primary particle, it is possible to extract some information of the environmental effects like atmosphere effect, geomagnetic field effect, atmosphere thickness effects, and so on. Since the effective parameters of the EAS events are so much, therefore we have to select them with their relative importance. From another side, the obtained information from ground based arrays of detectors is too limited to be able to investigate these effects well with their data sets. Also for more accurate and fine investigations, we need more accurate experiments and more statistics, which each of them have their limitations. Therefore in this part of the work, the role of simulations of EAS events will be very worthwhile. Actually, in our observatory the number and the type of our detectors have some limitations and some parts of it are not completed yet, like muon detectors and cosmic ray tracking (CRT) detectors, for the investigation of fine effects. So we need to investigate the effective and dominance factors on the EAS events separately and one by one via more accurate investigations of CORSIKA (COsmic Ray SIMulation for KAscade) [1] simulations. CORSIKA is a detailed Monte Carlo program to study the evolution of EASs in the atmosphere initiated by various cosmic ray particles. The prediction of particle energy spectra, densities, and arrival times to be observed in EAS experiments is a well suited application of CORSIKA. In this work the atmosphere thickness effect on the number of secondary particles was investigated where its details are as follows:

- (1) investigation $dN_{\text{sp}}(\theta, X)/d\theta$, where $N_{\text{sp}}(\theta, X)$ is the number of secondary charged particles in EASs as a function of atmosphere depth, X , and zenith angle, θ , and then to obtain $N_{\text{sp}}(X)$ in terms of X ,
- (2) to fit the function distribution $\sin\theta\cos^{n(X)}\theta$ to simulation data of $dN_{\text{sp}}(\theta, X)/d\theta$ and then to obtain the power index, $n(X)$, in different depths, X ,
- (3) to compare $n(X)$ obtained by CORSIKA simulation with the experimental data of various observatories.

II. GENERATION OF CORSIKA SIMULATION EVENTS

CORSIKA was originally developed to perform simulations for the KASCADE experiment at Karlsruhe [2,3] and it has been refined over the past few years. An important task in EAS Monte Carlo simulation is to take into account all knowledge of high energy hadronic and electromagnetic interactions, although the most serious problem is the extrapolation of hadronic interaction to higher energies, which has not been covered by experimental data in accelerators yet. So CORSIKA provides few hadronic interaction models at high energies. In this work we invoked the QGSJET01 [4] to simulate high energy hadronic interactions. This model is very successful in explaining experimental results in the high energy range.

Present results have been obtained by coupling the QGSJET model (qgsjet01.f package) [4], for hadronic interactions above $E_{\text{lab}} > 80$ GeV, and GHEISHA (Gamma Hadron Electron Interaction SHower code) [5] for interactions below this energy. For our Monte Carlo data library, we have simulated more than 10^5 showers in the energy range from 50 TeV to 5 PeV with an energy slope of -2.7 without thinning, and proton as primary particle. We simulated these EAS events based on the characteristics of our site (ALBORZ observatory) [6] i.e. altitude 1200 m above sea level (a.s.l.) with the magnetic field $B_x = 28.1 \mu\text{T}$ and $B_z = 38.4 \mu\text{T}$, which were obtained from U.S. Geomagnetic Data Center [7]. These simulations were carried out for different directions, with zenith angle, θ ,

*bahmanabadi@sina.sharif.edu

from 0° to 60° , and azimuth angle, ϕ , from 0° to 360° . The information of number of particles is available in produced files with suffix Lst in CORSIKA outputs. We used these files to ascertain the number of secondary charged particles in terms of different depths, X , and different arrival angles of primary particle.

III. ANGULAR DISTRIBUTION OF SECONDARY CHARGED PARTICLES IN DIFFERENT ATMOSPHERE DEPTH

Figure 1 shows the distribution $dN_{sp}(\theta, X)/d\theta$ for eight atmospheric depths. These distributions are quite different, which is related to the effect of atmosphere. We calculated $N_{sp}(X) = \int_0^{\pi/3} d\theta dN_{sp}(\theta, X)/d\theta$ for 45 atm depths.

Figure 2 shows $N_{sp}(X)$ as a function of X . These data have been obtained by 78782 EAS events. We fitted the function

$$N_{sp}(X) = \exp(a + bX^{1/2} \ln X + c \ln^2 X), \quad (1)$$

on the 45 obtained points which are number of secondary particles in 20, 40, ..., 900 g/cm² depths. In Eq. (1) a , b , and c are 7.4604, -0.1294 , and 0.8401 , respectively. As it is seen the shower maximum is at $X_{max} \approx 380$ g/cm². We also obtained the distribution of the secondary particles vs θ , for depths from 20 to 900 g/cm² by steps of 20 g/cm². By fitting the function $dN_{sp}(\theta, X_i)/d\theta \propto \sin\theta \cos^{n(X_i)}\theta$, where $X_i = 20i$ g/cm² with i from 1 to 45, on 12 points (from 0 to 60°) in each depth we obtained distribution

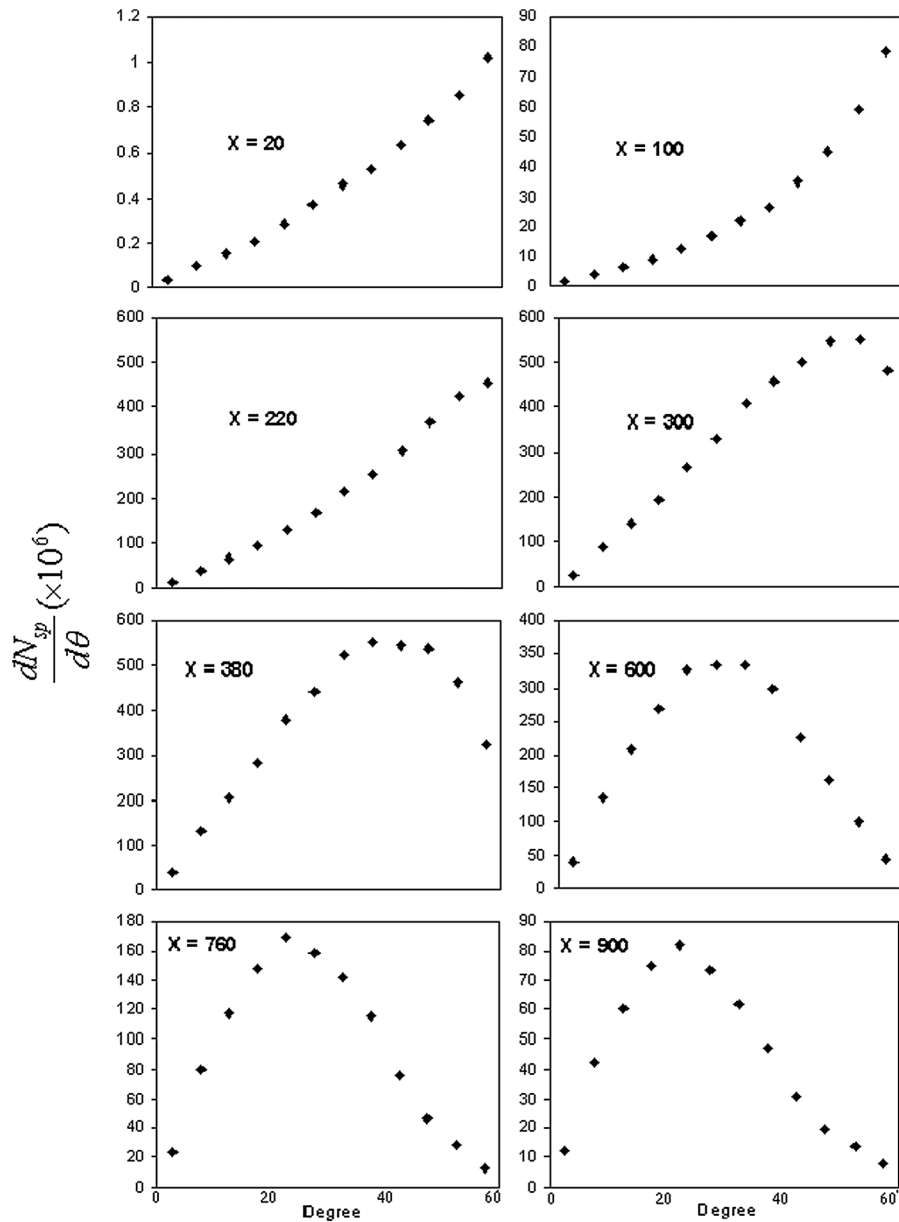


FIG. 1. Zenith angle distribution of secondary charged particles in different atmosphere depths.

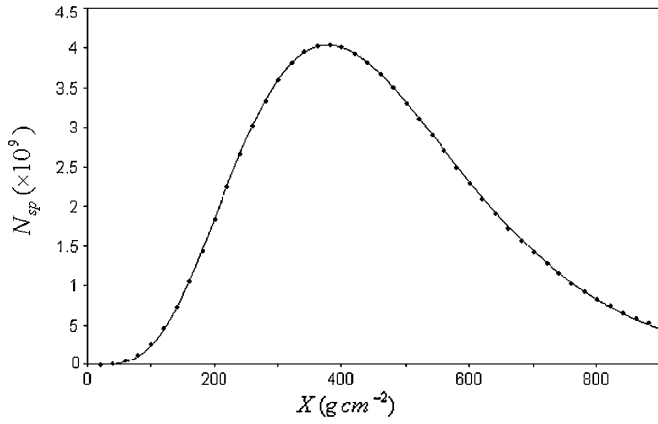


FIG. 2. Total number of secondary charged particles in different atmosphere depths.

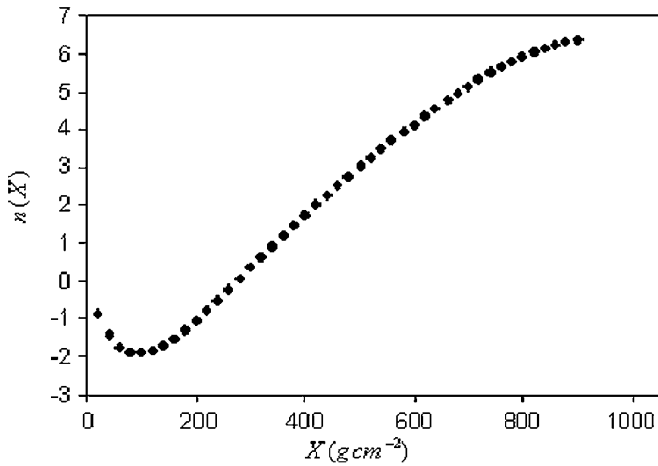


FIG. 3. The values n in terms of the atmosphere depth.

$n(X_i)$. The distribution is shown in Fig. 3. These points may be useful for the sites higher than our site, because the data of our simulations are saved until 1200 m a.s.l. (890 g/cm²). Meanwhile for observatories with low altitude (i.e. the depths greater than our site), we are able to calculate $n(X)$ using showers that are started with the zenith angle θ greater than zero. In the next section, we explain our method for determining $n(X)$ with $X > 900$ g/cm².

IV. DETERMINATION OF $n(X)$ AT THE ATMOSPHERE DEPTHS MORE THAN OUR OBSERVATORY DEPTH

When a shower event traverses through the atmosphere with a zenith angle, θ , it travels through an effective amount of matter of $X = X_0/\cos\theta$, where X_0 is the observed vertical depth. This event is equivalent with an event that is vertically entered to atmosphere but is observed at vertical depth X . Now if we go to an observation level that its vertical depth is X and take an event with a zenith angle θ' , its track length will be $X' = X/\cos\theta'$

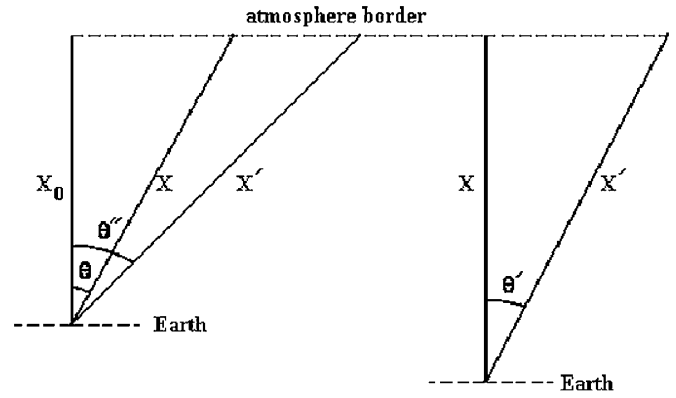


FIG. 4. Geometry definitions of slant thickness in vertical depths X_0 and X .

(Fig. 4). So we can write $X' = X_0/(\cos\theta' \cos\theta)$. If we again come back to the depth X_0 and we want to see such a depth, X' , we should choose zenith angle θ'' , so that

$$\cos\theta'' = \cos\theta \cos\theta'. \quad (2)$$

From the simulation data we have the distribution function $dN_{sp}(\theta'', X_0)/d\theta'' = A(X_0) \sin\theta'' \cos^{n(X_0)}\theta''$, and we want to make the distribution function $dN_{sp}(\theta', X)/d\theta' = A(X) \sin\theta' \cos^{n(X)}\theta'$ by the former distribution.

The default primary intensity distribution, I , in CORSIKA is

$$I \propto \sin\theta \cos\theta, \quad (3)$$

where the sin term respects the solid angle element of the sky, while the cos term takes the geometrical efficiency of a flat horizontal detector into account. With this assumption, we split $dN_{sp}(\theta'', X_0)/d\theta''$ as follows:

$$dN_{sp}(\theta'', X_0)/d\theta'' = \sin\theta'' \cos\theta'' f(\theta'', X_0), \quad (4)$$

with $f(\theta'', X_0) = A(X_0) \cos^{n(X_0)-1}\theta''$. $f(\theta'', X_0)$ depends only on the track length which is passed by secondary particles, i.e. $X_0/\cos\theta''$. Hence $f(\theta', X) = f(\theta'', X_0)$, and the distribution function $dN_{sp}(\theta', X)/d\theta'$ is calculated by the following formula:

$$dN_{sp}(\theta', X)/d\theta' = \sin\theta' \cos\theta' f(\theta'', X_0), \quad (5)$$

where $\theta'' = \cos^{-1}(\cos\theta \cos\theta')$. Therefore the procedure to obtain the distribution is performed as follows:

- Dividing $dN_{sp}(\theta'', X_0)/d\theta''$ by $\sin\theta'' \cos\theta''$ obtains $f(\theta'', X_0)$.
- By selecting θ and θ'' , and using $\cos\theta' = \cos\theta''/\cos\theta$, we obtain θ' .
- Finally, with multiplying the $\sin\theta' \cos\theta'$ by $f(\theta'', X_0)$, the distribution function $dN_{sp}(\theta', X)/d\theta'$ is obtained.

To test this method, four known levels, $X_0 = 840, 860, 880,$ and 900 g/cm², and for each level selected ten θ s ($\theta = 3^\circ, 6^\circ, 9^\circ, \dots, 30^\circ$) were examined. Then for each

X_0 , ten X s were generated. For example, with $X_0 = 840 \text{ g/cm}^2$ and $\theta = 21^\circ$, $X = 899 \text{ g/cm}^2$ was generated. We obtained $n(X) = 6.36$ while $n(X_0 = 900 \text{ g/cm}^2)$ is 6.34. So the calculation results are clearly consistent with the straight results of CORSIKA. On the other part for a special X using different X_0 s, we obtained $n(X)$. All of the $n(X)$ s are compatible with each other. For example, with $X_0 = 900 \text{ g/cm}^2$ and $\theta = 21^\circ$, $X = 964 \text{ g/cm}^2$ was generated and we obtained $n(X) = 6.36$. Also with $X_0 = 860 \text{ g/cm}^2$ and $\theta = 27^\circ$, $X = 964 \text{ g/cm}^2$ was again generated and we obtained $n(X) = 6.38$. So this method is self-consistent. Therefore we completed the $n(X)$ graph up to $X = 1039 \text{ g/cm}^2$.

V. RESULTS AND ANALYSIS

Figure 5 shows the power index, $n(X)$, as a function of X up to $X = 1039 \text{ g/cm}^2$. It is seen $n(X)$ becomes maximum at $X_{\text{max}} = 930 \text{ g/cm}^2$ and minimum at $X_{\text{min}} = 100 \text{ g/cm}^2$, which their values are $n(X_{\text{max}}) = 6.48$ and $n(X_{\text{min}}) = -1.9$, respectively. The best fit function to data is

$$n(X) = a + bX \ln X + cX^3 + d \ln X, \quad (6)$$

where $a = 3.02$, $b = 0.003$, $c = -8.28 \times 10^{-9}$, and $d = -1.35$.

Table I shows some experimental data of $n(X)$ at different atmosphere depths and in different energy ranges. We have compared the results of CORSIKA simulation with the experimental data of various observatories in the energy ranges which have been considered (Fig. 5). We have obtained the results calculated by the CORSIKA simulation are comparable with the measurements. The main uncertainty in the air shower simulations comes from our limited knowledge of the initial hadronic interactions, which take place at energies far exceeding those that can be observed

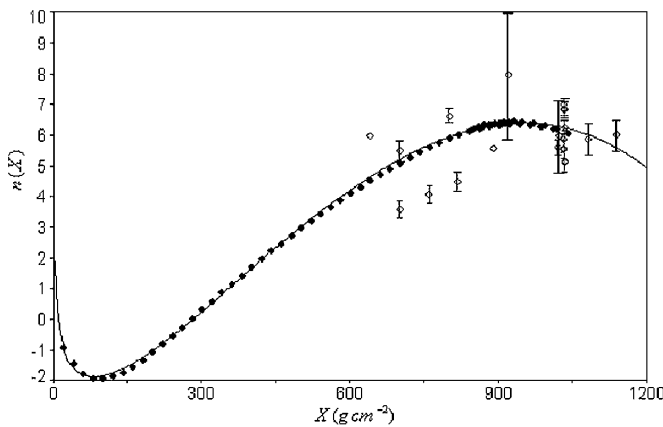


FIG. 5. The values n vs the atmosphere depth up to $X = 1039 \text{ g/cm}^2$; the solid curve shows the best fit function. Open circles show the experimental data which their origins are, respectively, from left to right and up to down as follows: 11, 20, 16, 20, 8, 20, 6, 20, 20, 17, 13, 13, 15, 13, 14, 15, 14, 14, 14, 14.

in the laboratory. Hence, the differences may be associated with peculiarities of the interaction models, but this matter needs more scrutinizing. In order to know sensitiveness to the particle composition, we used 78 782 proton showers and 36 405 alpha showers to produce $dN_{\text{sp}}(\theta, X)/d\theta$ for each type of shower separately. In this function X takes values of 20, 40, ..., 900 g/cm^2 . Then, with assuming 87% for proton and 13% for alpha, we obtained a mixed input

TABLE I. Some experimental data n in different energy ranges.

n	$X \text{ (g/cm}^2\text{)}$	Energy range (TeV)	log (shower size)	Reference
6.634 ± 0.1506	800	$10^2\text{--}10^4$...	[8]
7.05 ± 0.02	604	>0.1	...	[9]
5.58	890	>100	...	[6]
$6.90 \pm .01$	604	>100	...	[10]
6	639	>100	...	[11]
15 ± 1.2	1030	...	5–6	[12]
5.6 ± 0.4	1030	...	5–5.2	[13]
5.9 ± 0.5	1030	...	5.2–5.4	[13]
7.0 ± 0.3	1030	...	5.4–5.6	[13]
7.4 ± 0.7	1030	–	5.6–5.8	[13]
7.6 ± 0.6	1030	...	5.8–6	[13]
6.9 ± 0.3	1030	...	6–6.2	[13]
7.3 ± 0.4	1030	...	6.2–6.4	[13]
7.3 ± 0.3	1030	...	6.4–6.6	[13]
6.7 ± 0.3	1030	...	6.6–6.8	[13]
5.18 ± 0.36	1034	<i>knee</i>	...	[14]
5.90 ± 0.48	1080	<i>knee</i>	...	[14]
6.03 ± 0.52	1139	<i>knee</i>	...	[14]
6.53 ± 0.68	1219	<i>knee</i>	...	[14]
6.26 ± 0.69	1300	<i>knee</i>	...	[14]
5.16 ± 0.28	1034	[14]
6.28 ± 0.21	1034	...	5.15	[14]
6.86 ± 0.19	1034	...	5.35	[14]
8.04 ± 0.25	1034	...	5.65	[14]
7.97 ± 0.33	1034	...	6.05	[14]
7.88 ± 0.35	1034	...	6.15	[14]
7.97 ± 0.83	1034	...	6.35	[14]
5.56	1030	$<knee$...	[15]
6.86	1030	$<knee$...	[15]
5.5 ± 0.3	700	...	5.25	[16]
6.01 ± 1.20	1022	...	5.5	[17]
3.69 ± 0.30	820	<i>knee</i>	...	[18]
2.31 ± 0.54	700	<i>knee</i>	...	[19]
2.91 ± 0.17	700	<i>knee</i>	...	[20]
3.32 ± 0.18	758	<i>knee</i>	...	[20]
3.72 ± 0.24	816	<i>knee</i>	...	[20]
3.62 ± 0.20	700	<i>knee</i>	...	[20]
4.11 ± 0.22	758	<i>knee</i>	...	[20]
4.50 ± 0.27	816	<i>knee</i>	...	[20]
5.63 ± 0.21	1020	<i>knee</i>	...	[20]
8 ± 2.08	920	[21]

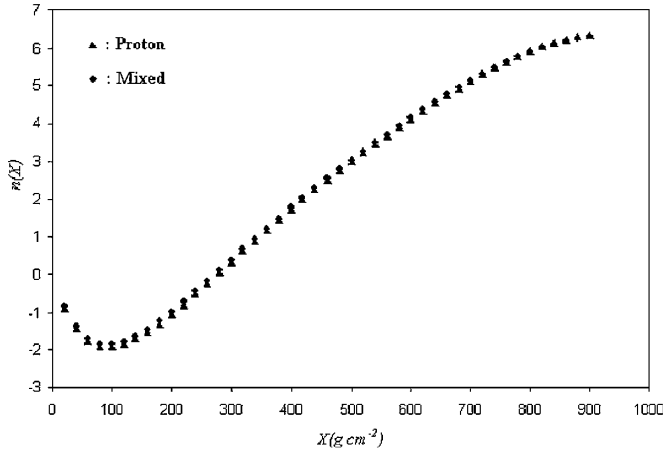


FIG. 6. The values n vs the atmosphere depth, obtained as a mixed input composition of proton and alpha particles (circles), and only proton (triangles).

composition and determined $n_{\text{mixed}}(X)$ in different depths and compared it with $n_{\text{proton}}(X)$. Figure 6 shows the comparison. If we define $\Delta n = |n_{\text{mixed}}(X) - n_{\text{proton}}(X)|$, we will have the following relations:

- (a) If $20 \text{ g/cm}^2 \leq X \leq 420 \text{ g/cm}^2$ then $0.04 \leq \Delta n(X) \leq 0.07$.
- (b) If $420 \text{ g/cm}^2 \leq X \leq 900 \text{ g/cm}^2$ then $0.00003 \leq \Delta n(X) \leq 0.04$. This is a more important range than the previous range, because it contains atmospheric depths of locations of all observatories.

Because the differences between the two functions are very small, we use $n_{\text{proton}}(X)$ representing both $n_{\text{proton}}(X)$

and $n_{\text{mixed}}(X)$. Therefore we omit the indexes and call them $n(X)$. In any case, since it is necessary to know carefully the value n for the other analyses of EASs, we need more scrutinizing in theory and experiment. The energy range of our simulations is 50 TeV–5 PeV, while that is a part of our energy range in the different experiments. This may be a part of the discrepancies.

VI. CONCLUSION

The study of the zenith angle distribution of extensive air showers is an important subject in order to deduce overall properties of the propagation of air showers through the atmosphere. The study makes us available to derive the attenuation length of the particle cascade. It is also a routine check for EAS arrays performance. So to examine the zenith angle distribution by an array with both good angular resolution and good statistics can be useful on the physical processes and improving them that are used in Monte Carlo simulations. We simulated more than 10^5 EAS events by CORSIKA code. The power index, $n(X)$, in the zenith angle distribution $\sin\theta \cos^{n(X)}\theta$ vs atmosphere depth, X , has a good fit with a regression analysis of better than 0.999 in the form $n(X) = 3.02 + 0.003X \ln X - 8.28 \times 10^{-9}X^3 - 1.35 \ln X$.

ACKNOWLEDGMENTS

This research has been partly supported by Grant No. NRCI 1853 of National Research Council of Islamic Republic of Iran. We are indebted to the anonymous referee for his numerous constructive comments.

- [1] D. Heck *et al.*, Report No. FZKA6019 (Forschungszentrum Karlsruhe), 1998.
- [2] T. Antoni *et al.* (KASCADE Collaboration), Nucl. Instrum. Methods Phys. Res., Sect. A **513**, 490 (2003).
- [3] K.H. Kampert *et al.* (KASCADE Collaboration), in Proceedings of the 26th ICRC, Salt Lake City, USA (1999), p. 159.
- [4] N.N. Kalmykov and S.S. Ostapchenko, Yad. Fiz. **56**, 105 (1993); Phys. At. Nucl. **56**, 346 (1993); N.N. Kalmykov, S.S. Ostapchenko, and A.I. Pavlov, Izv. RAN Ser. Fiz. **58**, 21 (1994); Bull. Russ. Acad. Science (Physics) **58**, 1966 (1994); Nucl. Phys. B, Proc. Suppl. **52**, 17 (1997).
- [5] H. Fesefeldt (GHEISHA Collaboration), Report No. PITHA-85/02, RWTH, Aachen, Germany, 1985 (unpublished).
- [6] M. Khakian Ghomi, M. Bahmanabadi, and J. Samimi, Astron. Astrophys. **434**, 459 (2005).
- [7] <http://www.ngdc.noaa.gov/seg/potfld/geomag.html>, 2002.
- [8] J. Cotzomi *et al.*, Rev. Mex. Fis. **51**, 38 (2005).
- [9] G. Di Sciascio *et al.*, J. Phys. Conf. Ser. **39**, 487 (2006).
- [10] G. Di Sciascio, E. Rossi (ARGO-YBJ Collaboration), arXiv:0710.1945.
- [11] A. Chilingarian *et al.*, Astropart. Phys. **25**, 269 (2006).
- [12] P. Bassi, G. Glark, and B. Bassi, Phys. Rev. **92**, 441 (1953).
- [13] Y.H. Tan *et al.*, in Proceedings of the 21st International Cosmic Ray Conference, 1990, Vol. 3, OG 6.2-16, p. 142.
- [14] K. Ghosh, S.K. Sarkar, and R.K. Chhetri, in Proceedings of the 29th International Cosmic Ray Conference, 2005, Vol. 6, p. 149.
- [15] D. Ciampa and R.W. Clay, J. Phys. G **14**, 787 (1988).
- [16] J.N. Capdeviellet *et al.*, J. Phys. G **20**, 947 (1994).
- [17] T. Antoni *et al.*, Astropart. Phys. **19**, 703 (2003).
- [18] M. Aglietta *et al.*, Astropart. Phys. **10**, 1 (1999).
- [19] A. Chilingarian *et al.*, Workshop ANI 99 (Report No. FZKA 6472, Forschungszentrum Karlsruhe, 1999), p. 43.
- [20] A. Chilingarian *et al.*, arXiv:astro-ph/0002076.
- [21] M. Nagano *et al.*, J. Phys. G **10**, L235 (1984).